Scale Adaptive Robotics

Bobins Augustine*, Arvind Selvan Chezhian, Gaetano Perchiazzi, Thiemo Voigt, Robin Augustine*

B.Augustine (ORCID : https://orcid.org/0000-0001-7224-3878), T.Voigt (ORCID : https://orcid.org/0000-0002-2586-8573)

Ångström Laboratory, Department of Electrical Engineering, Networked Embedded Systems, Uppsala University, Elektroteknik, Box 65,751 03, Uppsala, Sweden

R.Augustine (ORCID : https://orcid.org/0000-0002-2876-223X),A.Selvan Chezhian(ORCID:https://orcid.org/0000-0001-7593-0171)

Ångström Laboratory, Department of Electrical Engineering, Faculty of Solid-State Electronics, Microwaves in Medical Engineering Group, Uppsala University, Elektroteknik, Box 65,751 03, Uppsala, Sweden

G.Perchiazzi (ORCID : https://orcid.org/0000-0001-6834-6399)

The Hedenstierna Laboratory, Department of Surgical Sciences, Uppsala University, Akademiska sjukhuset, ing. 40 – tr. 3, 751 85, Uppsala, Sweden

Department of Anaesthesia, Operation and Intensive Care, Uppsala University Hospital, Akademiska sjukhuset, ing. 70 – tr. 1, 751 85, Uppsala, Sweden

E-mail: bobins.augustine@angstrom.uu.se, robin.augustine@angstrom.uu.se

Abstract

Scale Adaptive Robotics (SAR) represents a novel class of robots characterized by a ubiquitous design capable of adapting functional capabilities and physical interactions across different scales. This pioneering concept, introduced in this work, demonstrates how a bioinspired SAR design can be developed and implemented using scalable actuators fabricated through a hybrid additive process. SAR systems exhibit remarkable versatility, finding applications across varying scales. Miniaturized versions of these robots are suited for medical applications, such as intrabody drug delivery and in-vivo surgeries, while macro-scale counterparts are ideal for industrial and environmental uses, including soft grippers, robotic hands, and manipulators. This study showcases the size-dependent adaptability of SAR technology through the development of a fully biocompatible soft robot, illustrating its potential for both macro and micro applications. Importantly, the SAR concept is not constrained by the type of scalable actuator employed but relies on the functional design's ability to operate effectively across scales. By providing a scalable design template, SAR paves the way for advancements in fully automated robot manufacturing, offering transformative potential for diverse industries.

1. Introduction

Robotics is gaining unparalleled relevance, particularly in the healthcare industry, as the demand for medical systems with minimal human interaction grows because of increasing health risks due to global illness outbreaks happening in recent years [1,2]. Existing commercial robotic systems, such as the da Vinci® system (Intuitive Surgical), Mako™ system (Stryker Orthopaedics), CyberKnife® (Accuray Radiosurgery), Renaissance® Surgical Guidance System (Mazor Robotics Neurosurgery), and ViRob/TipCAT (Microbot Medical), demonstrate the potential of robotic intervention but its widescale application remains limited by their high costs and rigid structures [3-5]. This challenge extends to other robotic systems used in

environmental and industrial sectors, where increasing complexity, integration challenges across industries and high initial investment costs limit its large-scale adoption [6,7]. The manufacturing, The operation and decommissioning of modern robots also have a far-reaching environmental footprint. Soft robotics presents a promising solution, offering advantages over traditional rigid mechanical systems as they are more compliant, lightweight, and capable of nature-like dexterity. If such devices can be eco-friendly and versatile by adapting to different applications at various scales while maintaining the same design structure, and can be generated through fully or hybrid additive manufacturing techniques, they would offer significant benefits. They would not only reduce costs but also make robotic-assisted treatments and applications more sustainable, customizable, accessible, and easier to integrate across industries. This gap in technology has led us to the development of Scale Adaptive Robotics (SAR). To the best of our knowledge, SAR presented in this article is the first concept of its kind ever developed to fully address these challenges through a novel approach to robotic design and scalability.

We define SAR as the ability of robots to adapt to diverse functions and applications across varying scales while preserving its single functional design. Developed entirely by us through hybrid additive manufacturing, SAR represents a significant paradigm that introduces size-dependent adaptability, enabling unprecedented versatility, sustainability and cost-effectiveness. It embodies a universal design approach allowing robotic systems to function

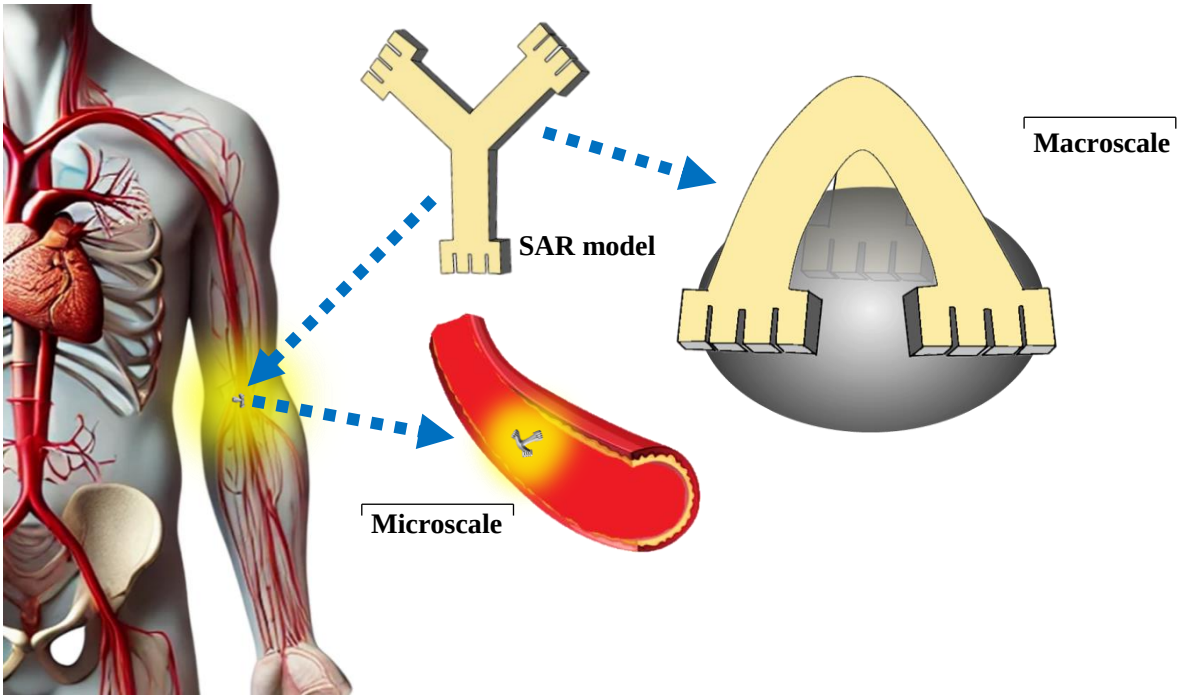

Figure 1. Depiction of the SAR concept illustrating size dependent versatility of the same scalable design for robots for different applications such as vascular robotics and a macro gripper.

seamlessly across various scales. SAR draws inspiration from the natural scalability observed in biological systems, where organisms grow in size while maintaining functionality. It is also inspired from the science fiction character "Ant-Man" from Marvel comics; When miniaturized, he can access narrow and confined spaces, while at larger scales, he exhibits enhanced physical strength to lift heavy objects. Similarly, SAR envisions robots capable of dynamically adapting their functionalities based on their dimensions. This inherent adaptability unlocks a wide range of possibilities, enabling applications in both miniature and large-scale robotics.

As this novel concept of SAR is first introduced in this work, we found certain capabilities that makes SAR useful for diverse applications in both macro and miniature scales. The three preferred capabilities for SAR are as following:

1. **Scalable Design:** Feature of a versatile design that maintains functionality across multiple scales. This design ensures seamless adaptability to varying dimensions without compromising performance, making the robot effective in both miniature and macro-scale applications**.**
2. **Locomotive Gait**: Possessing the ability to move and potentially in a manner that mimics any natural gait patterns observed in living organisms. This capability allows the robot to navigate its environment effectively, deliver items, whether in complex human-centric spaces or specialized industrial or environmental settings.
3. **Gripping Functionality**: The robot´s capability to hold or grip objects, enabling it to perform tasks that require functional capabilities, such as assembling components, delivering items, or even conducting surgical procedures.

For example, in Figure 1, the robotic system when scaled down, can navigate narrow vascular channels in the human body for drug delivery or precise surgical interventions. Conversely, when scaled up, the same system can function as a versatile soft gripper or manipulator for industrial or environmental tasks. This flexibility is at the core of SAR, where functionality is defined by a universal design template applicable across the micro to macro spectrum. Through hybrid or fully additive manufacturing techniques, SAR scalable robotic systems can be produced on demand [8], offering a high degree of flexibility and efficiency. Storing of the SAR designs in the digital cloud reduces the need for extensive physical inventory and significantly lowering the associated costs. This capability to manufacture robots as needed, rather than relying on large inventories, represents a significant advancement in cost-efficiency and responsiveness to market demands. Moreover, SAR design templates can

incorporate various scalable actuators, such as shape memory alloys (SMA), shape memory polymers, elastomers, electroactive polymers, liquid crystal elastomers, piezoelectric elements, and magnetic actuators [9,10]. Thus, the implementation of SAR is not limited by the type of scalable actuator.

In addition to enhancing manufacturing efficiency, SAR technology enables a new paradigm of adaptability in robotic applications. This adaptability allows for tailored and cost-effective solutions to meet specific needs, whether in the medical or environmental field—where accessibility, precision and biocompatibility [11] are crucial and in industrial contexts, where durability and dexterity are paramount [12]. The same robotic design can seamlessly transition from micro-scale surgical tools to macro-scale grippers, all while maintaining the desired functionalities tailored to each application. This approach can foster innovation across industries, creating opportunities for developing specialized robots that can perform a wider array of tasks with enhanced efficiency. For instance, in environmental monitoring, adaptable robots can access and analyze hard-to-reach areas within ecosystems, enabling better data collection and analysis. In the automotive and heavy machinery industries, SAR robots could conduct inspections and maintenance in narrow channels typically inaccessible with traditional tools, thereby improving operational efficiency and reducing downtime.

This article presents a proof of concept for SAR technology, demonstrating its scalability and versatility through a biocompatible robotic system. For the experiments in this work, we used nitinol-based SMA actuators due to their biocompatible and ease of processing nature. The system has been developed as a fully bio compatible miniature robot useful as an intrabody robot designed to operate within the simulated simplistic Y-split model symbolizing human vascular system, in view of application such as drug delivery and surgery. In this proof of concept work, the robot is made in millimeter scale to represent its miniature scale applications and we will focus in further miniaturization to very small dimensions in our future works. We use the term “microscale” in this proof of concept work to represent the miniature scale and small weight and in our future works we will be focusing on further miniaturization to lower dimensions. The same robotic architecture, when in macroscale, can function as a soft gripper for industrial applications for handling fragile or sensitive objects and is demonstrated in this work. As the demand for adaptable, cost-effective robotic systems continues to grow, SAR offers a unique solution. By providing a single, scalable design that can be tailored to a wide range of applications, SAR not only enhances the functionality of robotic systems but also introduces a potential for a new level of efficiency in their production and deployment. This

makes our SAR approach very useful for the future of robotics, with the potential to transform how we handle variety of complex tasks across multiple industries.

2. Experimental section

2.1 Materials and Methods

The material chosen for soft robot's exoskeleton was Polydimethylsiloxane (PDMS) silicone polymer from Wacker (Elastosil ®). It ensured biocompatibility, flexibility and durability for our applications in this work. The soft body material was prepared by thoroughly mixing the polymer with a curing agent in a 10:1 ratio, followed by air drying at room temperature for 3 hours. The robot's endoskeleton, which also serves as its actuation system, consisted of Shape Memory Alloy (SMA) nitinol wires obtained from Peiertech (佩尔科技®). These wires, with diameters of 0.5 mm and 1 mm and a transformation temperature (Af) of 45 °C, were selected for micro and macroscale application. The materials were chosen from already commercially available products for the proof of concept. However, for practical applications, parameters such as Af can be optimized for specific purposes by tailoring the composition of the SMA through customized production methods. The actuation control for the robot's paddling and crawling gaits was managed by an Arduino UNO microcontroller (ARDUINO®) and relay switching system (HF46F, Hongfa Europe GMBH), ensuring precise timing and movement sequences.

The SMA wires were thermally trained to achieve the desired bending deformations essential for locomotion. This training was conducted by mechanically bending the wires in predetermined directions and exposing them to a thermal treatment of 500 °C for 10 minutes using a Luxorparts Surface mount device station. This process allowed the wires to adopt a specific shape memory response. Upon current flow, the SMA wires heated due to ohmic losses, reaching their activation temperature and inducing the programmed bending actuation. When the current was deactivated, the wires returned to their relaxed state, and the natural elasticity of the polymer material facilitated their restoration to the straight configuration. This cyclical actuation, controlled by the microcontroller through periodic potential modulation, enabled the repeatable and synchronized movement patterns required for the robot's locomotion. The robot's individual limb movement was activated by the nitinol wires, while the return to the original position leveraged the polymer's inherent elasticity. For actuation, the miniature robot utilized

2.18V, 0.803mA, and 1.75W, while the macroscale robot utilized 2.58V, 3.17A, and 8.2W. The phase transition from martensite (disordered state) to austenite (ordered state) was achieved during thermal activation, inducing the desired bending actuation in the robot's limbs. The natural elasticity of the polymer facilitated the return of the legs to their original position after activation. Autonomous operation of the robot was achieved through programmed sequences in the Arduino UNO, with the delay required for the legs' relaxation, measured and integrated into the code.

2.2 Device Fabrication

The SAR soft robot was constructed using a hybrid additive manufacturing approach. The scalable design of the robot was modeled using SolidWorks CAD tools and fabricated using a ZYYX+ 3D printer. Both macro-scale and miniature-scale casts were printed. For this study, the macro-scale version of the SAR robot was set to 20 cm, while the miniature version was set to 40 mm in size. The shape-trained nitinol actuating wires, with diameters of 1 mm for the macro-scale version and 0.5 mm for the miniature version, were embedded into the 3D-printed casts. The wires were placed in precise locations for optimal actuation, the cavities were filled with the prepared soft body polymer and the cast was removed after air drying for 2 hours. The actuating wires were connected to power supplies via designated nodes, completing the assembly of the soft robot. The miniature version was programmed using an Arduino UNO to navigate through narrow crevices, while the macro-scale version was designed to function as a robotic gripper. Additionally, a 50 cm long Y- split channel representing vascular model was 3D-printed using Polylactic Acid (PLA) to simulate potential biomedical applications. The robot's contrasting sizes exhibited vastly different dynamics within its same design architecture, with the miniature version demonstrating its ability to operate within a PLA-based Y-split vascular structure and macro version as gripper.

2.3 Characterization

The characterization of the soft robot was performed using various electronic and mechanical tools to assess its electrical, thermal, and actuation performance. The electrical resistance of the nitinol actuators was measured using a precision digital multimeter, ensuring accurate calibration of the current required for SMA activation. The power supply used for the actuation tests was a programmable NICE-DC power supply, which provided stable voltage and current control to the SMA wires. The mechanical response of the robot, including the bending angles of the actuated limbs, was evaluated through a combination of videography and image analysis

to capture real-time motion dynamics. The integration and response times of the Arduino-controlled actuation system were further verified through real-time data logging, ensuring synchronized actuation and relaxation intervals essential for stable gait execution. Gait cycle analysis for the robot was monitored through stabilizing it with polar reference coordinate and recording images by temporal tracking of bending and extention angle of actuating legs with each gait cycle . The grasp and bending of the macroscale gripper were characterized using 2.2" Flex sensors from Electrokit Sweden AB (Malmö, Sweden). Flex sensors were also used for the arms. Bend angle was calculated by analyzing the resistance variation during the bending.

3. Results and Discussion

3.1 Design, simulation and implementation of the SAR robot

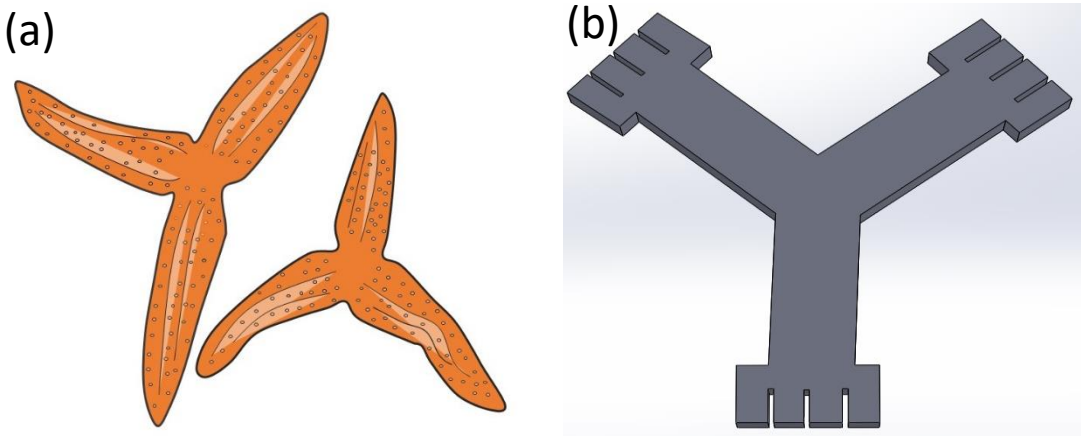

Figure 2. (a) Artistic rendering of divided state of allostichaster insignis starfish (b) Scalable template of the bioinspired SAR CAD model.

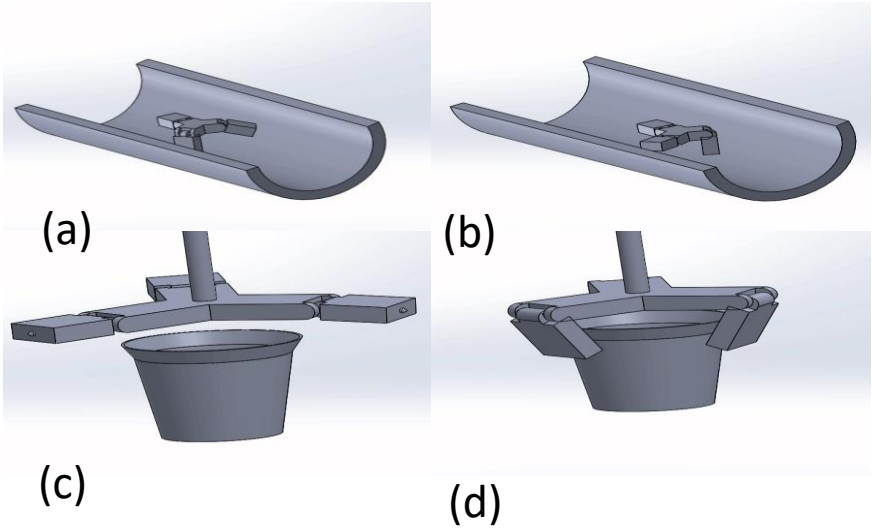

Figure 3. Simulation of SAR robot dynamics in different Scales. (a) &(b) Traversing gait through emulatory vascular Channel in miniature Scale for medical robotic application. (c) &(d) Gripping action in macroscale

A bio-inspired design based on the structure of allostichaster insignis starfish [13] during its division, is used as a scalable template for realizing SAR concept. The macroscale version has the dynamics of a gripper, the design is intended to grasp object with closing and opening motion with the

possibility of individual control of each finger. In its miniature version, the same design can translate like a bio organism moving through a given environment. Although inspired by the starfish, the design also mimics the functional movement of an octopus, particularly its ability to crawl using its limbs. It resembles specifically the behavior of the Octopus marginatus species, which demonstrates bipedal locomotion using its limbs. The structure is designed so that the front two legs or arms are utilized for locomotion, while the hind leg is dedicated to controlling direction and providing stability. The typical design is represented in Figure 2.

Before the physical construction of the SAR robot, simulations were employed to analyze the robot's actuation gait across microscale and macroscale conditions. These simulations served as a crucial step in validating the design's feasibility, ensuring that the proposed mechanisms functioned effectively within the constraints imposed by scale-dependent dynamics. The kinematic behavior of the SAR robot was modeled to understand its range of motion, and biomechanical mimicry, ensuring smooth adaptability across scales. Simulations also enabled optimization of energy efficiency by identifying potential inefficiencies in energy transfer. Additionally, material analyses were performed for the selection of materials and ensuring mechanical stability. The design process of the SAR robot was carried out in SolidWorks, where the CAD model was divided into its primary components to streamline the development and analysis. The overall simulation dynamics are presented in Figure 3. In microscale application modeling, the central component was the root leg, also functioning as

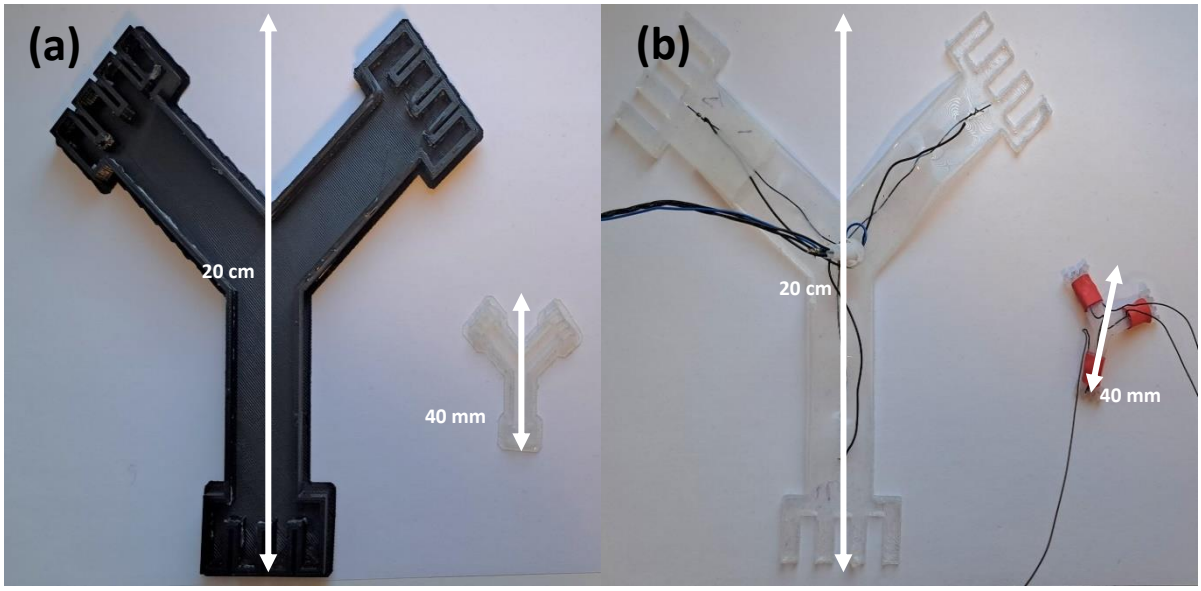

Figure 4. Hybrid additive manufacturing of SAR robot (a) 3-D printed cast of SAR CAD model, macro version (20 cm) and miniature version (40 mm) (b) SMR soft robots obtained from the cast molding with trained nitinol actuators embedded inside and connected wires for power supply.

the stabilizing limb, while the remaining two legs were designed to demonstrate the robot's

paddling gait. Each of these legs was further divided into two individual CAD parts, connected by a revolute joint mechanism designed to replicate the motion induced by SMA-based actuation. In the SolidWorks assembly, these individual components were integrated into a cohesive single entity. The assembled model was then subjected to gait motion analysis and boundary conditions, enabling a comprehensive simulation of its dynamic behavior and functionality. At the microscale level, the robot's design and subsequent motion analysis were performed to evaluate and understand the gait characteristics, such as step cycle, joint articulation, and motion efficiency of the SAR robot. Meanwhile, at the macroscale, a functional gripper design was developed and analyzed to demonstrate the robot's grasping capabilities during actuation. The simulations also facilitated the customization of actuation parameters, enabling the SAR robot to adapt its performance to specific operational requirements. The validation process of the SAR design model included testing its performance in virtual simulations of applications, both kinematically and dynamically. The results from this simulation helped to optimize the performance before manufacturing. The physical implementation of the design was achieved through hybrid additive manufacturing process and it is illustrated in Figure 4.

3.2 Kinematic Modelling for SAR robot

The kinematic analysis and modelling are essential for obtaining proper gait and stability of a robotic system. The general dynamics of the Asterina inspired SAR robot design is represented below in Figure 6. The paddling locomotion of the robot is formed by alternate bending of left and right arm of the robot together with root leg and gripping function is achieved through simultaneous activation of both sections together with root leg.

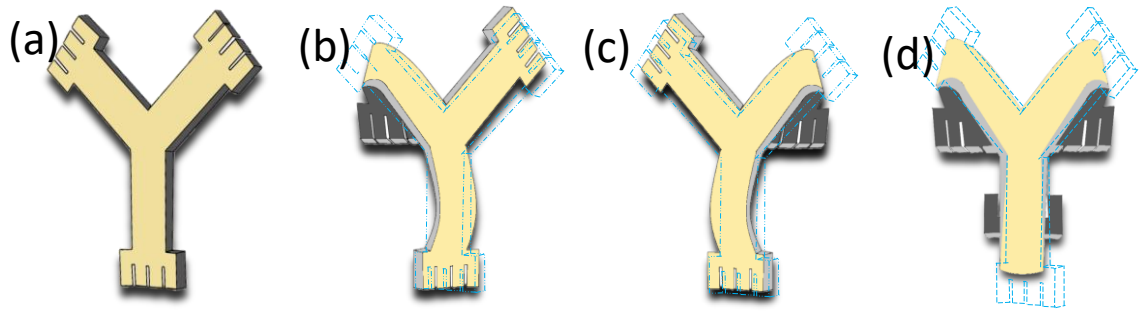

Figure 6. SAR dynamics (a) Reference position (b) left arm bending in paddling locomotion (c) right arm bending in paddling locomotion (d) gripping motion when all sections are activated simultaneously.

The forward kinematics of the robot is represented in Figure 7. It is used to solve the space position of the mechanical end effector and obtaining homogeneous transformation matrices

when angles of the three joints are known. The bioinspired "Y" shaped SAR architecture can be considered to have a common root leg and additional two identical front arms that split in to opposite direction. SMA-based nitinol actuators are used to drive the robot in this work. These actuators act as the endoskeleton of the robot. Nitinol actuators incorporated are trained such that they will have directional revolute joints to bend each limb, so the single section as in Figure 7 (a) is a Revolute-Revolute-Revolute joint in the kinematic system. Each joint has one degree of freedom. As the left and right sections of the structures are identical, solving one section is sufficient and streamlines the overall kinematics model. The gripping kinematics is equivalent to simultaneous activation of both sections.

In order to facilitate the foreward kinematics of the actuating limbs of the robot, the Denavit Hartenberg (DH) [14] coordinate system as in Figure 7 (b) is established. To achieve a streamlined model as mentioned earlier, we have focused the kinematic analysis on the single section, as illustrated in Figure 7(c), since all sections are identical. The coordinate O_0-$X_0Y_0Z_0$ is the base of root leg and is fixed as the origin. The coordinate O_1-$X_1Y_1Z_1$ is attached at the joint between root leg and Arm 1, the coordinate O_2-$X_2Y_2Z_2$ is fixed on the elbow part of the Arm 1. The coordinate O_3-$X_3Y_3Z_3$ is attached at the end effector. In a DH system, the number of the coordinate frames can be generally represented as n. The angle θ_n is the angle of rotation around the axis Z_{n-1} to align X_{n-1} with X_n. The angle α_n represents the twist angle around axis X_n to align Z_{n-1} with Z_n. The parameter l_n is the offset distance along X_n. The parameter d_n is the offset distance along Z_{n-1}.

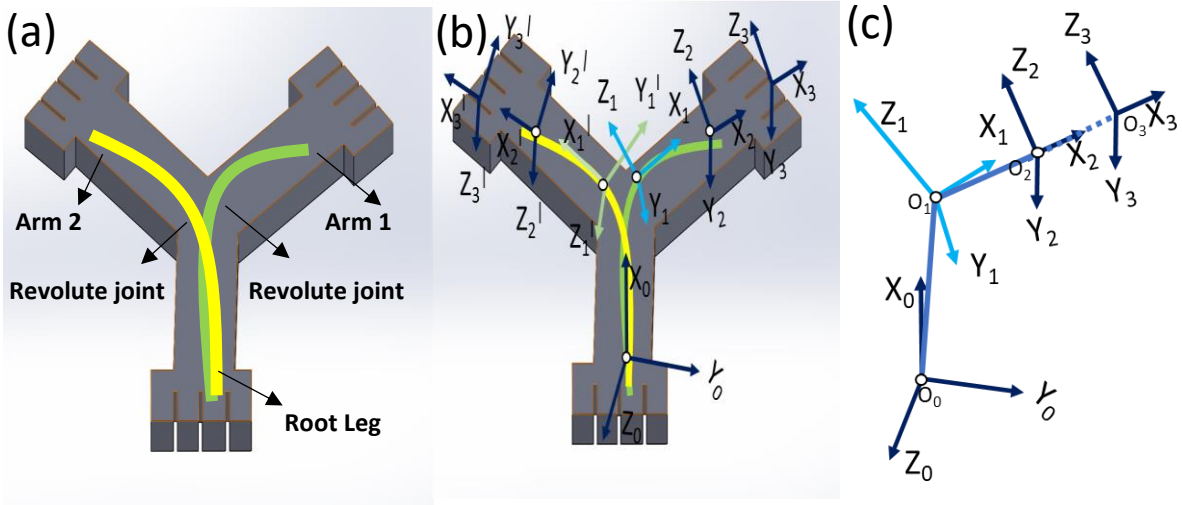

Figure 7 (a) Structure of Asterina inspired SAR, Green and Yellow lines indicate trained nitinol actuator wires (b) kinematics diagram of the robot (c)DH coordinate diagram, (Root Leg to Arm 1 dynamics) in a three-frame system.

The representative D-H parameters for the 3-frame system is shown below. It includes two rotation angles and two displacement parameters.

n	θ_n	α_n	l_n	d_n
1	θ_1	α_1	l_1	d_1
2	θ_2	α_2	l_2	d_2
3	θ_3	α_3	l_3	d_3

Table 1. D-H system

For deriving homogeneous transformation matrix for foreward kinematics, in each joint, we derive transformation matrix Tn-1, n using D-H parameters.

Transformation matrix from Frame n-1 to n is given by,

$$T_{n-1,n} = \begin{bmatrix} \cos\theta_n & 0 & \sin\theta_n & l_1\cos\theta_n \\ \sin\theta_n & 0 & -\cos\theta_n & l_1\sin\theta_n \\ 0 & 1 & 0 & 0 \\ 0 & 0 & 0 & 1 \end{bmatrix}$$

Transformation from Frame 0 to 1 (T_{01})

$$T_{01} = \begin{bmatrix} \cos\theta_1 & 0 & \sin\theta_1 & l_1\cos\theta_1 \\ \sin\theta_1 & 0 & -\cos\theta_1 & l_1\sin\theta_1 \\ 0 & 1 & 0 & 0 \\ 0 & 0 & 0 & 1 \end{bmatrix}$$

.

Transformation from Frame 1 to 2 (T_{12})

$$T_{12} = \begin{bmatrix} \cos\theta_2 & -\sin\theta_2 & 0 & l_2\cos\theta_2 \\ \sin\theta_2 & \cos\theta_2 & \mathbf{0} & l_2\sin\theta_2 \\ 0 & 0 & 1 & 0 \\ 0 & 0 & 0 & 1 \end{bmatrix}$$

.

Transformation from Frame 2 to 3 (T_{23})

$$T_{23} = \begin{bmatrix} \cos\theta_3 & -\sin\theta_3 & 0 & l_3\cos\theta_3 \\ \sin\theta_3 & \cos\theta_3 & 0 & l_3\sin\theta_3 \\ 0 & 0 & 1 & 0 \\ 0 & 0 & 0 & 1 \end{bmatrix}$$

Overall transformation from frame 0 to frame 3:

The complete transformation from base (0) to the end effector frame (3) is obtained by multiplying the individual transformation matrices.

$$T_{03} = T_{01} * T_{12} * T_{23}$$

Each transformation matrix is multiplied in sequence to yield the final transformation matrix that describes the position and orientation of the end effector relative to the base frame. The final matrix T_{03} allows us to determine the foreward kinematics for the asterina inspired robot by relating the joint angles and lengths to the end -effector position.

3.3 Control circuit for the SAR robot

The control system designed for the miniature robot is a closed looped system and for the macroscale gripper, it is an open loop system driven by external input. Below is the representation of the control circuit. The microcontroller modulates the flow of current in the

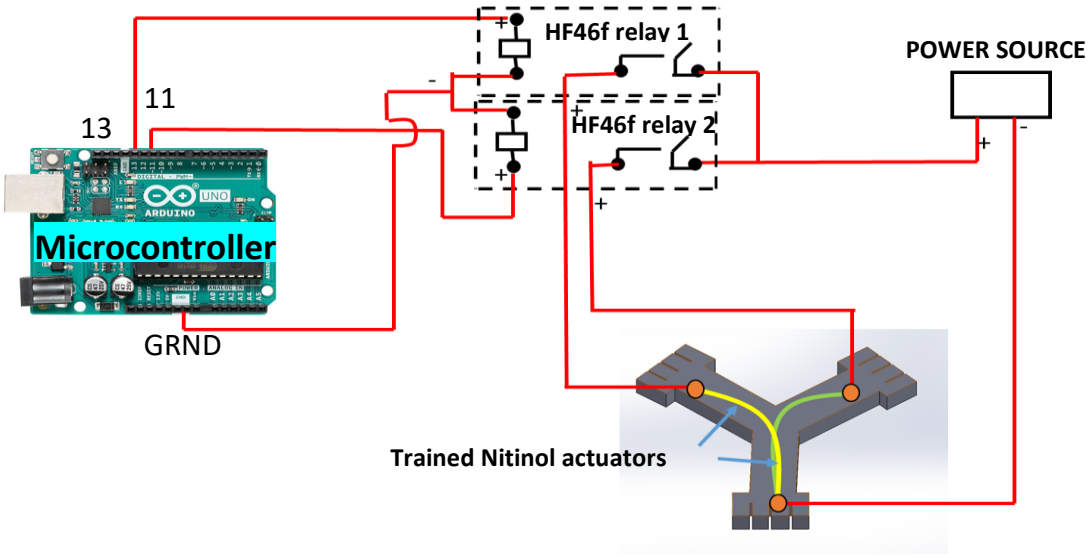

Figure 5. Illustration of the driver Circuit of SMR robot using Arduino UNO microcontroller.

two front alternative arms and hind root leg. The switching is achieved through the relay system with. The digital signals from pin 11 controls the left arm to root leg section and signals from pin 13 controls right arm to root leg section. To attain gripping motion, both pin 11 and 13 are activated simultaneously to create bending motion in root leg and front arms.

3.4 Combined effect of Exo and Endo Skelton on actual kinematics

The dynamic behavior of the robot arises from the interaction between its soft polymer exoskeleton and shape memory alloy (SMA) endoskeleton. The soft exoskeleton provides the necessary elastic restoring force to counteract and recover from the bending motion induced by

the SMA endoskeleton. Furthermore, due to the physical connection of the arm via the exoskeleton, the bending motion of one arm generates a lateral pulling force on the adjacent arm. This results in cumulative motion dynamics [15] driven by the interplay between the endoskeleton actuation and the elastic forces exerted by the exoskeleton.

3.4.1 Actuating gait under polar coordinate tracking

To analyze the gait cycle in locomotion, the robot is stabilized in a polar coordinate frame. The root leg is fixed in the frame so that the robot can be tracked for its consistent motion as in Figure 8.

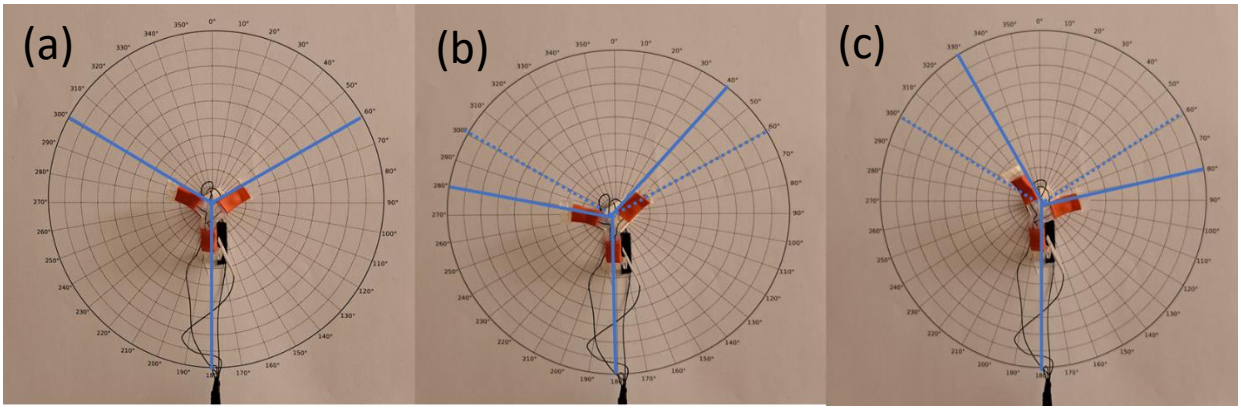

Figure 8. Acuating gait cycles (a) Reference position (b) 1st cycle with left arm bending and simulatneous extension of right arm (c) 2nd cycle with right arm bending with simulatneous extension of left arm.

The robot´s locomotion of paddling gait is a repetition of the first and the second cycle of gaits. In the first gait cycle, the robot´s left arm is bend and right arm is extended and in second cycle, the right arm is bend and the left arm is extended. In the first cycle and second cycle, when the activating arm is bend, it will have a pull on the relaxed non-activated arm due to the physical connection through polymer. This happens for the root leg as well, however to understand the true nature of the consistent gait, the root leg is stabilised in the coordinate so that the locomotion pattern can be extracted without errors. The robot pattern in locomotion adapts to the surface it is treading on or navigating. The root leg or the hind leg acts like a stabiliser that motivate the robot to force the foreforeward movement.

The gait cycle is analysed further in the plot analysis in Figure 9. The gait cycle plot visualizes the locomotion dynamics, with the red line representing the left arm and the blue line representing the right arm of the robot. Positive values correspond to arm bending, while negative values indicate arm extension or relaxation. The actuation begins with the left arm during the first gait cycle, followed by the right arm in the second cycle.

Subsequent gait cycles alternate between these motions. It can be observed from the plots that during left arm activation, it bends by 20°, while the right arm simultaneously extends by 20° from its reference position. Conversely, the right arm during activation also bends by 20°, but the left arm extends by 30° from its reference position. This pattern is observed consistently for

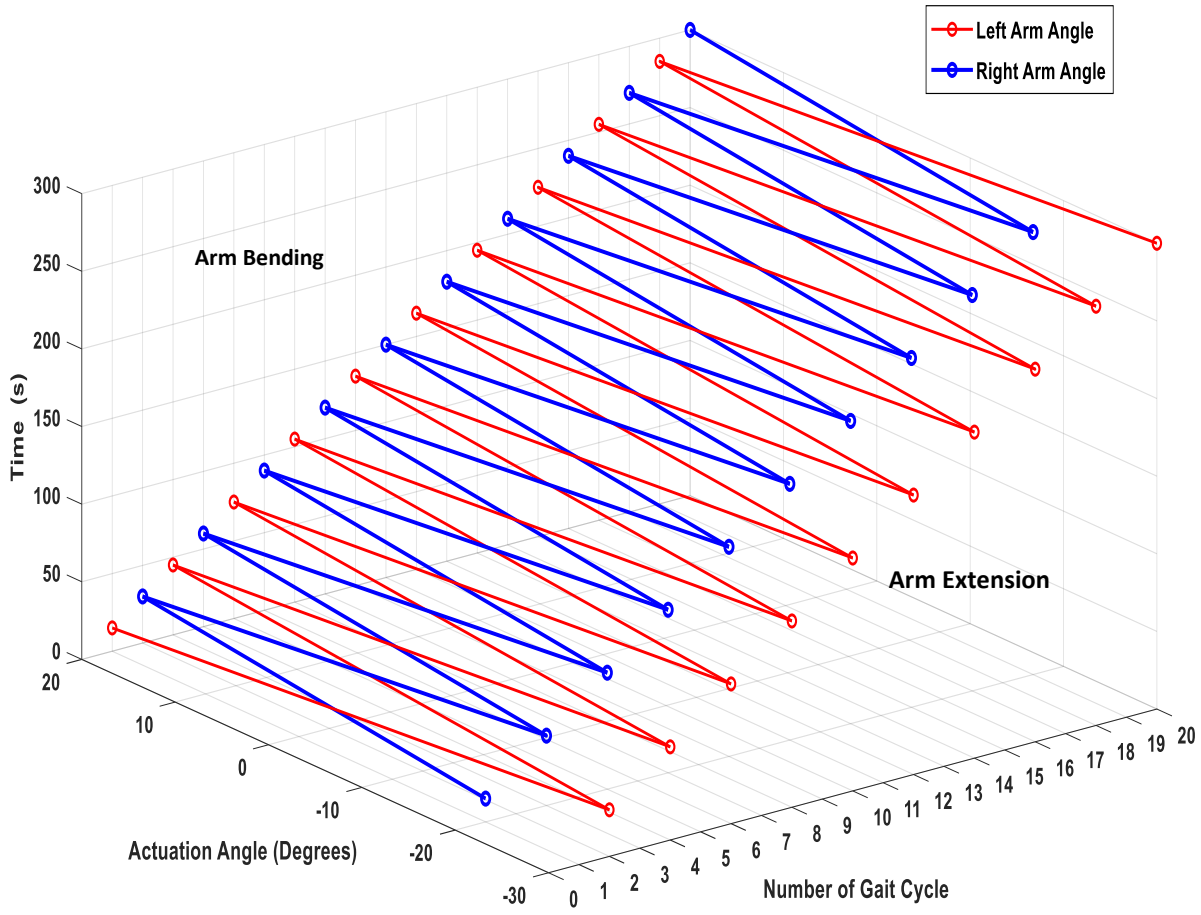

Figure 9. Plot analysis of gait cycle

all gait cycles. We attribute the angle asymmetry in left arm extension and right arm extension to the combined effects of the individual shape programming in SMA endoskeleton and the elastic properties of the PDMS polymer exoskeleton. This insight suggests that the robot's locomotion speed can be optimized by tuning the Young's modulus of the polymer and synchronized shape programming of the individual endoskeleton to achieve a balance between the elastic recovery force of the exoskeleton and the actuation force of the SMA [16,17]. Each gait cycle duration is also designed to allow sufficient recovery time for the non-activated arm, ensuring smooth and consistent motion.

3.5 Size dependent Applications

3.5.1 Vascular intrabody robot

Modern medical treatments often face significant challenges when addressing complex vascular conditions and delivering therapies to hard-to-reach areas within the body. For example, cardiovascular diseases, one of the leading causes of mortality worldwide, often necessitate the use of stents to restore blood flow in blocked arteries. While stents provide an immediate solution, they may come with long-term complications, including tissue overgrowth leading to restenosis and the calcification of vessels, which renders the vascular channels rigid and less functional [18,19]. These complications necessitate active interventions, which in turn can increase risks and costs for patients. In oncology, achieving precise delivery of chemotherapeutic agents directly to the tumor site is crucial for maximizing treatment effectiveness and improving patient outcomes.

Conventional catheter-based one-dimensional systems are often not effective in reaching precisely their target site, and this limits their therapeutic effectiveness. This lack of precision not only reduces treatment efficacy but also leads to systemic side effects that may compromise the patient's overall health [20,21]. Similarly, the treatment of calcified vessels poses unique challenges, as traditional methods rely on invasive surgical procedures that may not always be feasible for patients with compromised health.

These limitations highlight a critical need for advanced systems capable of navigating the vascular environments with high precision and minimal invasiveness. A robotic solution tailored for such applications which is complimentary to the current already established treatments could address these gaps by autonomously traversing vascular channels, enabling dynamic and localized interactions with the surrounding tissues. Such systems could deliver therapeutic agents directly to target sites, remove obstructions, or perform localized treatments without the need for open surgery. The benefits of this approach extend beyond vascular treatments. In cancer therapies, these systems could improve drug delivery, enabling higher therapeutic concentrations at the tumor site while minimizing systemic exposure. Additionally, they could play a vital role in diagnosing and treating vascular anomalies without the rigidity associated with long term structure reinforcement-based interventions, preserving the natural flexibility of the vessels.

To validate the proof of concept of SAR as miniature intrabody robotic solution that can travel through narrow crevice’s inside human body, the robot is tested in a simulated bifurcated

channel as similar to a vascular channel. The channel is made by 3D printing PLA model of length 50 cm. The channel is filled with aquatic fluid dyed as red simulating the blood. The robot is then allowed to crawl through the channel as in Figure 10. The material choice for SAR robot was made specifically to satisfy this application. The robot itself is fully biocompatible [22,23] including the actuator endoskeleton and polymer exoskeleton. The robot traverses through the channel autonomously following feedback from the closed looped control system as mentioned previously. The directional hemodynamic flow of blood can also assist in the navigation of the microrobot, allowing it to reach targeted sites with precision.

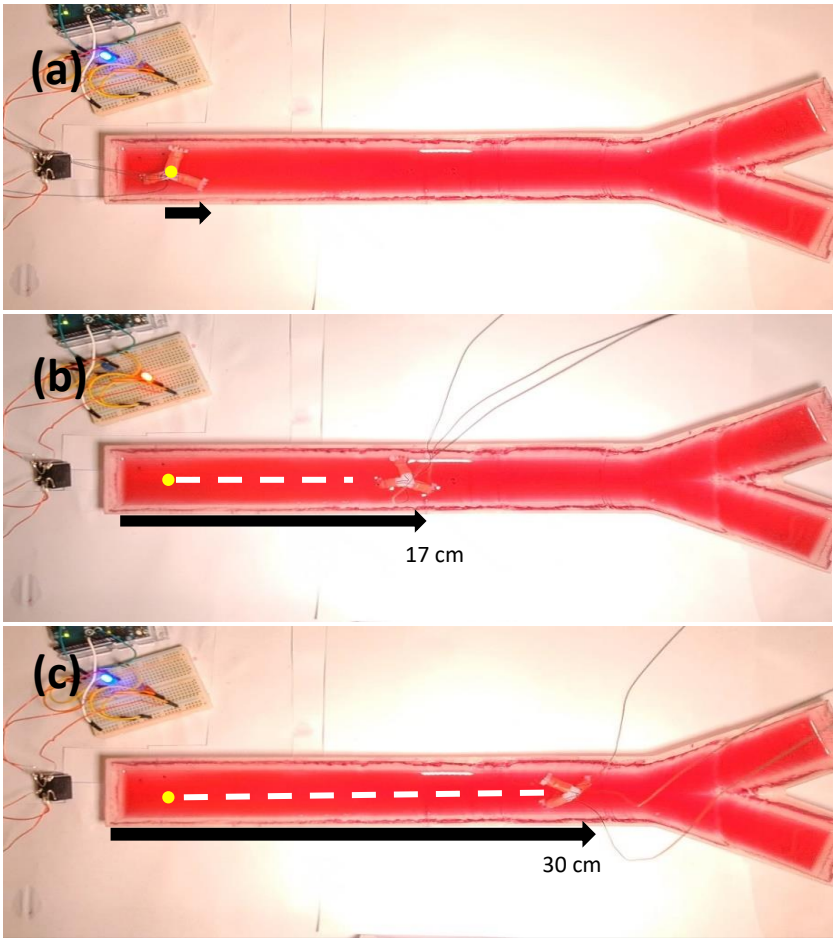

Figure 10. locomotion of miniature SAR robot demonstrating application in vascular robotics

As in the dynamic flow scenario, the blood flow itself can take the robot from one place to another and its limb movement is only needed to either pivot to a direction or stabilize itself in a location. Thus, in applications where rapid movement is less critical than controlled actuation, the focus shifts to optimizing the leg movement patterns to facilitate precise functional tasks. The integration of tethered systems also offers substantial benefits for SAR applications in biomedical settings. Tethering not only provides continuous power but also enables the safe retraction of the microrobot, thereby simplifying operational logistics. The robot can also work as a fully mobile robot with integration of miniature battery or power harvesting module. This system can be enhanced in our future works by incorporating conformal antennas to support high-bandwidth communication for data-intensive applications. Such configurations enable

real-time feedback, enhancing the robot's responsiveness during surgical procedures, which is crucial for maintaining operational integrity and efficacy. The advantage of this system is that it can seamlessly compliment current catheter-based treatment systems where the miniaturized intrabody robot could be launched through it and work in collaboration with the existing treatment methods. This intrabody miniature robot can be also used to access other cavities inside human body such as lungs and intestines where it can carry out targeted treatments.

3.5.2 Macroscale Soft Grippers

Soft grippers have emerged as indispensable tools in various industries due to their unique ability to handle delicate, irregularly shaped, and fragile objects that traditional rigid grippers struggle with [24-27]. Their inherent flexibility and adaptability make them ideal for applications such as food processing, where they can grasp and handle without causing damage, and also in electronics manufacturing, where precision and care are paramount. Agriculture is one of the most hazardous sectors in both the United States and Canada, with high rates of injuries and fatalities [28]. Due to rising labor demands, many countries have to rely on migrant workers and these workers also suffers other factors like low wages, health issues caused by excessive heat and humidity, and the repetitive nature of tasks that require uncomfortable body positions [29-32.]. For example, in the case of harvesting fragile and high-value crops still demands substantial manual labor [33]. It is reported that in Dutch greenhouse farming, the total expense spent on human labor can cost up to €300,000 [34] annually per business and the problem is growing due to a global shortage of workers in agriculture. This need is increasing as the industry shifts from mass production to a focus on specialized methods aimed at improving the quality of crops. For instance, Italian farmers who have embraced precision farming report a higher labor demand than those who have not [35]. Automation through robotic grippers and manipulators presents a potential solution to all these challenges.

By integrating cost-effective and efficient robotic systems, farmers could reduce their reliance on human workers, lower operational expenses, and improve their profit margins. The integration of Scale Adaptive Robotics (SAR) into soft gripper technology enhances these capabilities by introducing scalability, allowing the same unique design to be easily adjusted for different sizes and operational scales without compromising performance. This adaptability is particularly advantageous when produced through hybrid or fully additive manufacturing for industries that deal with diverse product dimensions or require customization for specific tasks. The proof of concept of the macroscale application of SAR robot is illustrated in Figure11.

Each arm was also tested with flex sensors [36] to measure the angle of bend to hold the object correctly.

The dynamic relationship of these parameters was analyzed and the plot is demonstrated in Figure 12. The angle of bend using flex sensor is calculated using the following equation

$$\mathbf{R = m \cdot \theta + R_0}$$

$$m = (\mathbf{R_{180} - R_0})/(\mathbf{180 - 0})$$

Where **R** = resistance at bend angle θ (kΩ), **m** = slope, $\mathbf{R_{180}}$= resistance at 180° bending,

$\mathbf{R_0}$ = resistance at 0°, θ = bend angle (in degrees).

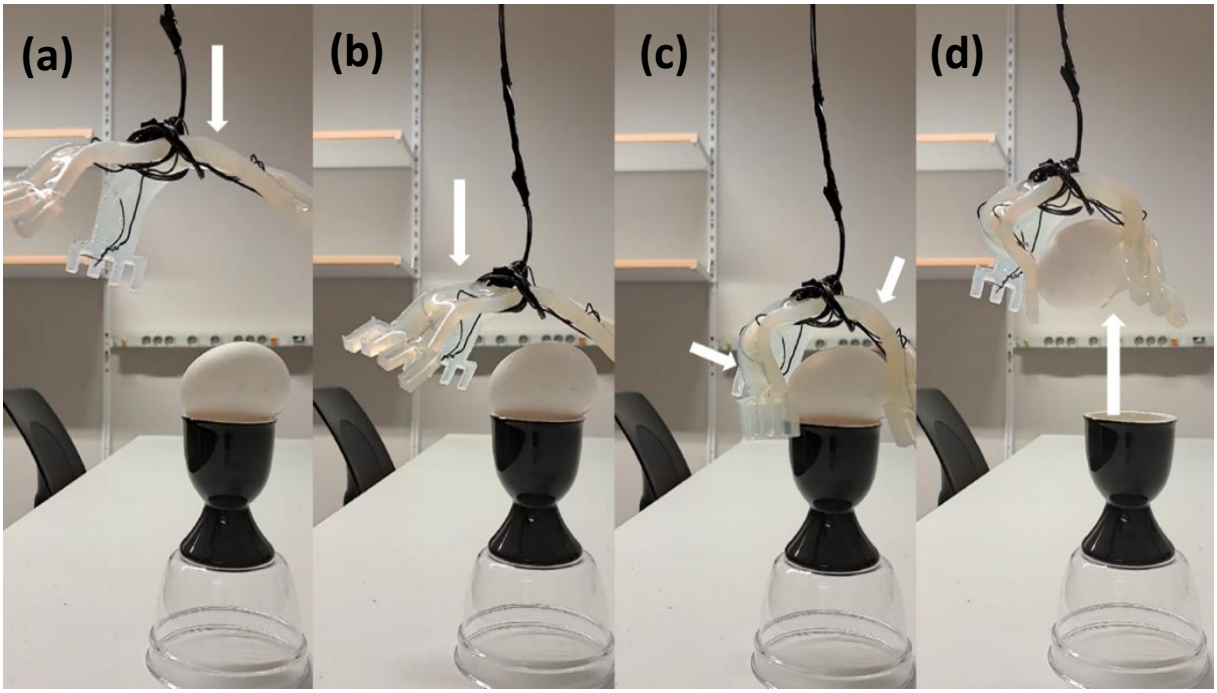

Figure 11. Demonstration of Macroscale application of the SAR robot in gripping function in picking up an egg.

The flex sensor showed R_0 resistance of 27.38 kΩ and R_{180} resistance of 124.7 kΩ . The bend angle of the arms when grasping the object was measured. During grasp, the root arm or root leg showed a bend resistance of 95.8 kΩ which is equivalent to 126. 8° bend angle, right arm (viewed from front) showed a bend resistance of 106.2 kΩ which is equivalent to 145.7° bend angle and the left arm (viewed from front) showed bend resistance of 102.4 kΩ which is equivalent to the bend angle of 139°.

In the soft gripper, the variation of the gripping angle might vary depending on the shape of the holding object, rigidity differences in arms during fabrication as well as the slight variation of

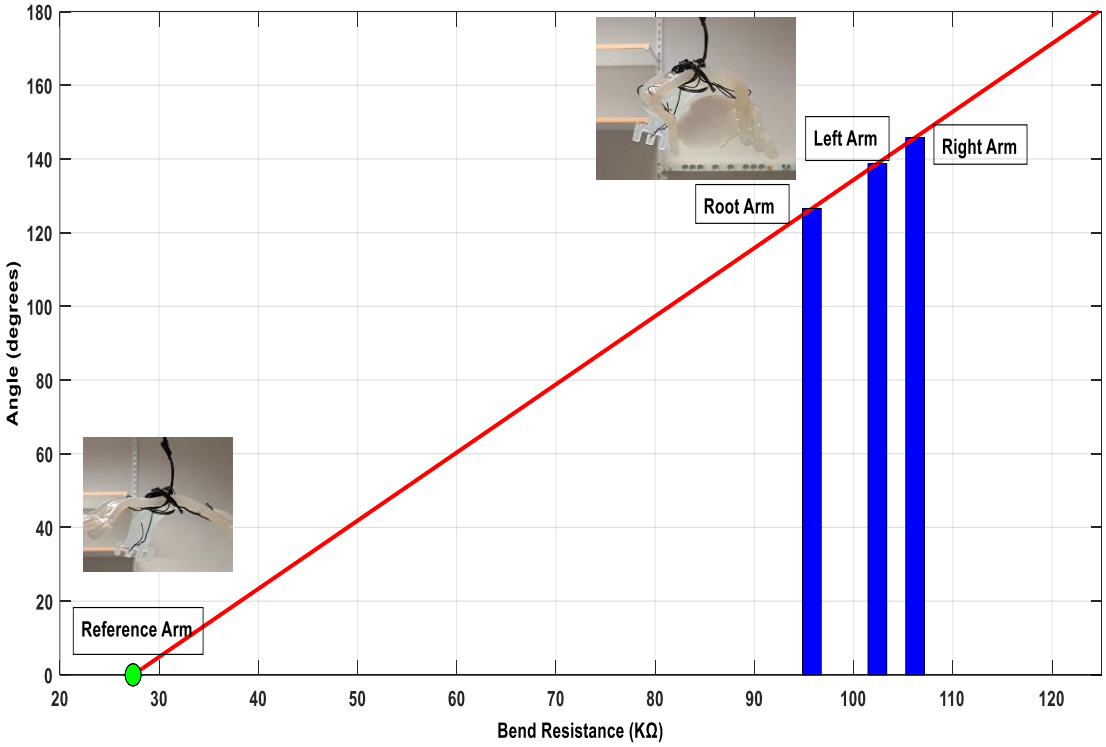

Figure 12. Plot showing bend resistance vs angle of grasping

how the nitinol actuators are programmed to bend. Further optimization in fabrication and actuator programming can provide enhanced synchronicity in gripping angles for all arms. The soft gripper in the experiment demonstrated to be efficient by successfully grasping the fragile object safely.

3.6 Advantages of SAR robotic system

A key advantage of SAR is its intrinsic scalability, which facilitates the application of a single robotic architecture in multiple environments. This scalability is not merely a function of size alteration; it fundamentally involves a design philosophy that prioritizes performance across micro to macro scales. In industrial settings, SAR robots can be deployed as manipulators capable of handling fragile components or conducting complex assembly tasks, demonstrating that a unified design can yield significant efficiency and cost savings. This approach mitigates the economic burden associated with maintaining extensive inventories, as SAR systems can be manufactured on demand using hybrid or fully additive manufacturing processes.

The adaptability of the SAR system not only demonstrates its functional range but also underscores its potential for cross-domain applications. By maintaining its structural principles and allowing flexibility in actuator choice, the design provides a robust platform that also

combines simplicity with performance. This scalability and design flexibility position the SAR system as a highly versatile tool in soft robotics, capable of addressing challenges across different fields without being constrained by the type of actuator employed. Converting such functional and scalable design for robot through additive manufacturing will reduce the cost of fabrication and simplify production. This will give added advantage to robots that can be produced on demand from designs stored in the cloud, which reduces expensive inventory and storage facilities. Using same intrinsic and scalable design for robotic systems that can have variety of applications including environmental, industrial and health care will have great positive influence on economy and society.

4. Conclusion

The novel SAR technology developed and presented in this article is highly relevant because it bridges the gap between scalability and adaptability, offering a unique solution for modern robotics. It is also demonstrated in this work that a fully biocompatible and sustainable soft robot is possible in the SAR method. By combining nature-inspired scalability, on-demand additive manufacturing, and flexible actuator design, SAR can revolutionize applications in the fields from medical, industrial and environmental. It introduces a new paradigm of robotic systems by adding versatility, paving the way for easy integration, efficient, and sustainable robotic applications across a wide range of fields. Building on this foundation, our further research will also explore and implement additional SAR designs to expand its transformative potential. SAR's ability to adapt in size and function with same design could truly transform how we approach robotics in the future.

Conflict of Interest

Bobins Augustine is the inventor on the filed patent on 12/06/24 (Intracavity robot, SE 2450648-7) and It covers this work including the locomotion, gripping functionality, application and use of various scalable actuators. Bobins Augustine and all other coauthors declare no conflict of interest.

Author Contributions

Bobins Augustine: conceptualization (lead); data curation (lead); investigation (lead); methodology (lead); software (lead); validation (lead); Visualization(lead); writing—original draft (lead); writing—review and editing (equal). **Arvind Selvan Chezhian:** Software (supporting) and data curation (supporting). **Gaetano Perchiazzi:** writing—review and editing

(equal). **Thiemo Voigt:** writing—review and editing (equal). **Robin Augustine**: conceptualization (supporting); funding acquisition and research resources (lead); investigation (equal); methodology (equal); writing—review and editing (equal); validation (equal).

Acknowledgments

This research was supported by the Swedish Foundation for Strategic Research (SSF) and Swedish Agency for Innovation Systems (Vinnova) in the Microbots for Drug delivery and monitoring Applications project-(BODEGA) (grant no. 2023-01451).

Data Availability Statement

The data that support the findings of this study are available from the corresponding author upon reasonable request.

Keywords

Soft robot, Scalable, Adaptive design, Autonomous, Biomimetic, Biocompatible

References

[1] Centers for Disease Control and Prevention (CDC), COVID-19 Timeline, https://www.cdc.gov/museum/timeline/covid19.html, accessed: January, 2025.

[2] World Health Organization (WHO), Disease Outbreaks News, https://www.who.int/emergencies/disease-outbreak-news, accessed: January, 2025.

[3] Cepolina F, Razzoli R J. Robot Surg. 2024, 18, 74.

[4] L. Lawrie, K. Gillies, E. Duncan, L. Davies, D. Beard, Marion K. Campbell, PLOS ONE 2022, 17, e0273696.

[5] C. BenMessaoud, H. Kharrazi, K. F. MacDorman, PLOS ONE 2011, 6, e16395.

[6] R.D.S.G. Campilho, F.J.G.Silva, Machines 2023,11, no. 11: 1011.

[7] M. Misaros, O.P. Stan, I.C. Donca, L.C. Miclea, Sensors 2023, 10, 4962.

[8] R. K. Mahapatra, Y. Kaliyath, N. S. V. Shet, G. S. Satapathi, S. R. Mahapatro, M. L. Naidu, Proc. Int. Conf. Intell. Cyber Phys. Syst. Internet Things (ICoICI) 2024, 528–532.

[9] X. Huang, M. Ford, Z. J. Patterson, M. Zarepoor, C. Pan, C. Majidi, J. Mater. Chem. B 2020, 8, 4539.

[10] T. Dayyoub, A. V. Maksimkin, O. V. Filippova, V. V. Tcherdyntsev, D. V. Telyshev, Polymers 2022, 14, 3511.

[11] M. Bernard, E. Jubeli, M. D. Pungente, N. Yagoubi, Biomater. Sci. 2018, 6.

[12] A. Grau, M. Indri, L. Lo Bello, T. Sauter, IEEE Ind. Electron. Mag. 2021, 15, 50.

[13] T. Rubilar, C. López, L. Pérez, Rev. Biol. Trop. 2005, 53, 337.
[14] J. Denavit, R. S. Hartenberg, J. Appl. Mech. 1955, 22, 215.
[15] C. Liang, C. A. Rogers, J. Vib. Acoust. 1993, 115, 129.
[16] S. Kumar, J. Mater. Sci. Mater. Eng. 2024, 19, 15.
[17] D. J. S. Ruth, J.-W. Sohn, K. Dhanalakshmi, S.-B. Choi, Sensors 2022, 22, 4860.
[18] P. Libby, et al., Circ. 2002, 105, 1135.
[19] G. M. Doherty, et al., Nat. Rev. Cardiol. 2012, 9, 237.
[20] R. K. Jain, Annu. Rev. Biomed. Eng. 1999, 1, 241.
[21] Z. Tang, et al., Curr. Opin. Biotechnol. 2019, 58, 160.
[22] I. Miranda, A. Souza, P. Sousa, J. Ribeiro, E. M. S. Castanheira, R. Lima, G. Minas, J. Funct. Biomater. 2022, 13, 2.
[23] K. Vrchovecká, J. Mrázková, M. P. Goldbergová, Metallomics 2022, 14, mfac002.
[24] M. Armada, P. Gonzalez-de-Santos, Sensors 2021, 21, 2689.
[25] P. Polygerinos, Z. Wang, IEEE Robot. Autom. Lett. 2015, 1, 1039.
[26] L. Wang, H. Ji, Sci. Robot. 2020, 5, eaaz5004.
[27] S. Gomez, P. Garcia, Autom. Sci. Eng. J. 2020, 25, 112.
[28] S. C. Moyce, M. Schenker, Annu. Rev. Public Health 2018, 39, 351.
[29] E. J. Van Henten, Acta Hortic. 2006, 710, 55.
[30] Y. Vecchio, G. P. Agnusdei, P. P. Miglietta, F. Capitanio, Int. J. Environ. Res. Public Health 2020, 17, 869.
[31] N. Popova, A. Rakotonarivo, Int. Labour Organ. Geneva 2021.
[32] F. Westhof, Rapport arbeidsmigranten 2021.
[33] R. MacCurdy, A. Parness, IEEE Trans. Robot. 2012, 28, 1186.
[34] G. Jukema, R. van der Meer, Agri-Monitor 2009, 11.
[35] J. Lowenberg-DeBoer, I. Y. Huang, V. Grigoriadis, S. Blackmore, Precis. Agric. 2020, 21, 278.
[36] S. Alapati, Int. J. Emerg. Technol. Adv. Eng. 2017, 7, 97.